Interface Sliding As Illustrated by the Multiple Quaternary Structures of Liganded Hemoglobin[†,‡]

Timothy C. Mueser,[§] Paul H. Rogers, and Arthur Arnone*

Department of Biochemistry, College of Medicine, The University of Iowa, Iowa City, Iowa 52242

Received June 6, 2000; Revised Manuscript Received September 14, 2000

ABSTRACT: Initial crystallographic studies suggested that fully liganded mammalian hemoglobin can adopt only a single quaternary structure, the quaternary R structure. However, more recent crystallographic studies revealed the existence of a second quaternary structure for liganded hemoglobin, the quaternary R2 structure. Since these quaternary structures can be crystallized, both must be energetically accessible structures that coexist in solution. Unanswered questions include (i) the relative abundance of the R and R2 structures under various solution conditions and (ii) whether other quaternary structures are energetically accessible for the liganded $\alpha_2\beta_2$ hemoglobin tetramer. Although crystallographic methods cannot directly answer the first question, they represent the most direct and most accurate approach to answering the second question. We now have determined and refined three different crystal structures of bovine carbonmonoxyhemoglobin. These structures provide clear evidence that the dimer−dimer interface of liganded hemoglobin has a wide range of energetically accessible structures that are related to each other by a simple sliding motion. The dimer−dimer interface acts as a "molecular slide bearing" that allows the two $\alpha\beta$ dimers to slide back and forth without greatly altering the number or the nature of the intersubunit contacts. Since the general stereochemical features of this interface are not unusual, it is likely that interface sliding of the kind displayed by fully liganded hemoglobin plays important structural and functional roles in many other protein assemblies.

Only in the case of an allosteric protein is more than one quaternary structure anticipated. Even in this case, it is usually stated or implied that the allosteric protein in question can adopt only two quaternary structures—one defined by a crystal structure of the unliganded form of the protein and the other by a crystal structure of the fully liganded protein. In terms of the notation of the general two-state allosteric model of Monod, Wyman, and Changeux (*1*), the quaternary structure of the unliganded protein is referred to as the "tense" T structure, and the quaternary structure of the fully liganded protein is termed the "relaxed" R structure. For many years the $\alpha_2\beta_2$ mammalian hemoglobin tetramer was thought to be a paradigm for an allosteric protein having two, and only two, quaternary structures. In large part, this view was held because the initial crystallographic evidence was compelling (*2*, *3*). Virtually identical quaternary structures have been observed in all the crystal structure determinations of deoxyhemoglobin reported to date, and until 1991 only one quaternary structure had been reported for fully liganded hemoglobin. The Protein Data Bank now contains the refined structures of two crystal forms of human wild-type deoxyhemoglobin (*4*−*6*), one of human sickle cell deoxyhemoglobin (*7*, *8*), one of bovine deoxyhemoglobin (*9*), and one of trout deoxyhemoglobin (*10*). In addition, the structure of human deoxyhemoglobin recently has been determined in a third crystal form that is grown from an unbuffered PEG solution of very low salt concentration (<1 mM) where the pH is approximately 7.1, the isoelectric point of hemoglobin (*11*). These six structures are characterized by essentially the same quaternary structure (the T structure) even though they were determined over a wide range of crystallization conditions (e.g., the salt concentration varies from ∼0 to >2.5 M) and in different crystal lattices. Likewise, very similar quaternary structures (the R structure) were reported in two independent crystal structure determinations of fully liganded hemoglobin, one of oxy (or carbonmonoxy) human hemoglobin (*12*, *13*) and one of horse methemoglobin (*14*). Since the residues that define the critical $\alpha1\beta2$ interface[1] are conserved in all mammalian hemoglobins, it was generally assumed that the T and R structures are the only energetically accessible quaternary structures for all mammalian hemoglobins (*15*).

In 1991, Smith et al. (*16*) reported a 3.0-Å crystal structure of the carbonmonoxy form of hemoglobin Ypsilanti, a mutant hemoglobin in which Asp99(G1)β^2 (a residue at the center

[†] This work was supported by Grants HL-51084 and GM-58890 from the National Institutes of Health. T.C.M. also was supported by postdoctoral fellowships from the National Institutes of Health (F32HL08740−01) and from the Iowa Cardiovascular Center.

[‡] Refined coordinates have been deposited in the Protein Data Bank. The accession numbers for the structures bHb·CO·PEG5.0, bHb·CO·HS7.2, bHb·CO·PEG8.5, and eHb·CO·HS8.5 are 1G08, 1G09, 1G0A, and 1G0B, respectively.

* To whom correspondence should be addressed. E-mail: arthur-arnone@uiowa.edu.

[§] Present address: Department of Chemistry, University of Toledo, Toledo, OH 43606.

[1] The notation $\alpha1\alpha2$, $\beta1\beta2$, $\alpha1\beta1$, $\alpha2\beta2$, $\alpha1\beta2$, and $\alpha2\beta1$ refers to the six subunit−subunit pairings within the $\alpha_2\beta_2$ hemoglobin tetramer.

[2] The amino acid residue notation includes the secondary structure position of a residue. Thus, Asp99(G1)β locates residue Asp99β as the first residue of the β subunit G helix.

10.1021/bi0012944 CCC: $19.00
Published on Web 11/21/2000

of the $\alpha 1\beta 2$ interface) is replaced by tyrosine. This crystal structure of liganded hemoglobin Ypsilanti has a quaternary structure (referred to as the Y structure) that is very different from both the R structure and the T structure. This was the first direct evidence that an $\alpha_2\beta_2$ hemoglobin tetramer can adopt a quaternary structure other than the R and T structures. However, the hemoglobin Ypsilanti mutation dramatically alters the thermodynamic properties of the hemoglobin tetramer. In terms of the equilibrium between $\alpha\beta$ dimers and the $\alpha_2\beta_2$ tetramer, this mutation destabilizes the deoxy tetramer by 5.7 kcal/mol and stabilizes the liganded tetramer by 3.3 kcal/mol (*17*). Thus, the liganded tetramer is more stable than the deoxy tetramer by 2.6 kcal/mol in hemoglobin Ypsilanti. In wild-type hemoglobin, the deoxy tetramer is more stable than the liganded tetramer by 6.3 kcal/mol (*18*). Of all the variant hemoglobins studied to date, only hemoglobin Ypsilanti has been found to cause a large inversion in the stability of the $\alpha 1\beta 2$ interface (*18*). For this reason, it has been argued that the quaternary structure of liganded hemoglobin Ypsilanti is mutation-induced and not representative of a quaternary structure that is populated to a significant level by wild-type hemoglobin (*19*).

Both the R structure of wild-type hemoglobin and the Y structure of hemoglobin Ypsilanti were determined from crystals grown under conditions of high-salt concentration at pH 6.7. In 1992, Silva et al. (*20*) reported a 1.7-Å structure of wild-type carbonmonoxyhemoglobin that was determined with crystals grown from a poly(ethylene glycol) solution at pH 5.8 under conditions of much lower salt concentration. Surprisingly, the quaternary structure of carbonmonoxyhemoglobin determined from these crystals (referred to as the R2 structure) is much closer to that of liganded hemoglobin Ypsilanti than to the R or T structures. Although important differences appear to exit between the Y structure and the R2 structure (*20*), the discovery of the R2 structure showed that the hemoglobin Ypsilanti mutation stabilizes an arrangement of the $\alpha 1\beta 2$ interface that is accessible to wild-type hemoglobin.

The discovery of the R2 structure encouraged us to carry out a more extensive search for other energetically accessible structures of liganded hemoglobin. In particular, we attempted to find conditions for producing well-ordered crystals of mammalian hemoglobins that have identical primary structures over the entire $\alpha 1\beta 2$ interface. The rationale behind this approach is that subunit−subunit interactions across the $\alpha 1\beta 2$ interface are the dominant factor in controlling the quaternary structure of the hemoglobin tetramer (*3*, *21*). Variation in surface residues, on the other hand, should have little impact on quaternary structure stability, but it could have a very large influence on the way in which a particular hemoglobin molecule crystallizes. For example, variation in one or more surface residues could alter the relative solubility of the R and R2 structures. If the R and R2 structures are the only structures that are energetically accessible to fully liganded hemoglobin in solution, only these structures should be observed in new crystal forms of liganded mammalian hemoglobins. If this is not the case, a screen of several crystal forms could reveal the existence of energetically accessible quaternary structures that differ from the R and R2 structures. In this paper, we report three structures of bovine carbonmonoxyhemoglobin as determined from three different crystal forms. One has a quaternary structure that is almost identical to the R2 structure of liganded human hemoglobin, but the other two have quaternary structures that are positioned between the R and R2 structures. Collectively, the ensemble of liganded mammalian hemoglobin structures shows that the $\alpha 1\beta 2$ interface acts as a "molecular slide bearing" that allows the two $\alpha\beta$ dimers to slide back and forth without greatly altering the number or the nature of the intersubunit contacts.

EXPERIMENTAL PROCEDURES

Notation. The notation for the various hemoglobin crystal forms has the following form: species·ligand·precipitant&pH. The species codes are hHb (human hemoglobin), bHb (bovine hemoglobin), and eHb (equine hemoglobin). The ligand codes are DX (deoxy), O_2 (oxygen), CO (carbon monoxide), and Met (aquomet). The precipitant codes are HS (high salt) and PEG (poly(ethylene glycol)). For historical reasons, the hHb·DX·HS6.8 (*6*), hHb·O_2·HS6.7 (*13*), and hHb·CO·PEG5.8 (*20*) crystal structures were chosen as the reference T, R, and R2 structures, respectively. The symbol R^e refers to the ensemble of liganded mammalian hemoglobin structures.

Crystallization of Bovine Carbonmonoxyhemoglobin at pH 5.0. Purified bovine hemoglobin (a gift from Dr. Hiroshi Ueno) was concentrated to 14% protein and stored as pellets at −80 °C. A variation of the crystallization conditions reported for the R2 structure of human carbonmonoxyhemoglobin (*20*) was used to produce large crystals of bovine carbonmonoxyhemoglobin. The best crystals (1.5 × 1.4 × 0.9 mm) grew from solutions of 2% bovine carbonmonoxyhemoglobin, 300 mM sodium cacodylate (prepared by titrating sodium cacodylate with HCl to pH 5.0), 2 mM sodium dithionite (added to eliminate methemoglobin formation), and 11.5% Dow PEG 3350. These crystals were grown from 200-μL batch setups in a nitrogen-filled glovebox with stock solutions that had been purged with CO. CO also was injected into each crystallization vial.

Crystallization of Bovine Carbonmonoxyhemoglobin at pH 8.5. Bovine hemoglobin was purified from whole blood according to the procedure described by Perutz (*22*), concentrated to 16% protein, and stored as pellets at −80 °C. Prior to crystallization, aliquots of hemoglobin were thawed, purged with CO, and then deionized with a Dintzis column using the procedure described by Riggs (*23*) with the addition of a 1-mm layer of CHELEX resin (iminodiacetic acid, Sigma Catalog No. C-7901) placed on the top of the column.

The pH 8.5 crystal form of bovine carbonmonoxyhemoglobin was produced with the following screening strategy. The screening method utilizes 4 anionic buffers, 12 ionic additives, and 1 precipitating agent to prepare a total of 48 crystallization solutions. The four buffers were MES at pH 5.8, PIPES at pH 6.5, HEPES at pH 7.5, and TAPS at pH 8.5. The 12 ionic additives were the ammonium salts of formate, acetate, phosphate, sulfate, citrate, and cacodylate and the chloride salts of ammonium, sodium, potassium, lithium, magnesium, and calcium. Each buffer and each additive was used at a final concentration of 100 mM. Additives having significant buffer capacity were titrated to pH 5.8, 6.5, 7.5, or 8.5 with ammonium hydroxide or hydrochloric acid. The precipitating agent was Dow PEG 3350 at a final concentration of 25%.

Table 1: Data Collection and Refinement Statistics

	eHb·CO·HS8.5	bHb·CO·HS7.2	bHb·CO·PEG5.0	bHb·CO·PEG8.5
	Data Collection			
space group	C2	$P2_12_12_1$	$P2_12_12_1$	$P2_12_12_1$
unit cell				
a (Å)	108.8	64.4	79.4	73.8
b (Å)	63.2	160.2	110.9	131.6
c (Å)	54.6	55.3	66.2	63.1
β (deg)	110.7	90	90	90
asymmetric unit	dimer	tetramer	tetramer	tetramer
resolution (Å)	1.9	2.0	1.9	2.0
measurements	316,145	210,904	334,873	304,865
unique reflections	25,974	36,539	45,723	38,865
completeness (%)	97.5	96.1	96.8	96.0
R_{merge} (%)	4.6	7.1	5.8	6.7
	Refinement			
R_{cryst} (%)	17.8	19.9	19.6	18.9
water molecules	74	118	95	145
rms of bond lengths (Å)	0.10	0.008	0.009	0.009
rms of angle distances (Å)	0.024	0.022	0.023	0.023
average temp factor (Å^2)	24.8	27.5	31.2	26.9

Hanging drop setups were prepared using two 24-well Linbro trays with 400-μL reservoir solutions and 8-μL drops prepared from 4 μL of 4% carbonmonoxyhemoglobin and 4 μL of the reservoir solution. Within a few days, it was possible to determine by visual inspection the anion and cation additives and the pH that produced the best crystals. At the best pH, a series of second screens was carried out by varying the PEG concentration and by using mixtures of the ammonium and chloride salts of the best anion and cation. For bovine carbonmonoxyhemoglobin, several conditions for crystallization were found in the first screen with the best crystals growing from solutions containing ammonium sulfate or potassium chloride. Large rod-shaped crystals (2.5 $\times$ 0.8 $\times$ 0.6 mm) were grown in one of the second screens from solutions of 4% bovine carbonmonoxyhemoglobin, 100 mM TAPS (pH 8.5), 50 mM ammonium sulfate, 200 mM potassium chloride, and 19% PEG 3350.

Crystallization of Bovine Carbonmonoxyhemoglobin at pH 7.2. In this case, bovine carbonmonoxyhemoglobin (prepared as described above for the pH 8.5 crystals) was crystallized under high-salt conditions similar to those used to crystallize human carbonmonoxyhemoglobin (*22*). Batch setups of 2% carbonmonoxyhemoglobin in 2.5−2.0 M sodium/potassium phosphate (a total volume of 200 μL) were prepared in 1-mL shell vials, purged with CO, and sealed. A large well-formed single crystal (1.3 $\times$ 0.3 $\times$ 0.3 mm) was cleaved from a cluster of crystals and used for data collection. Crick reported preliminary X-ray studies on an isomorphous high-salt crystal form of bovine carbonmonoxyhemoglobin in 1956 (*24*).

Crystallization of Horse Carbonmonoxyhemoglobin at pH 8.5. Horse carbonmonoxyhemoglobin (prepared as described for bovine carbonmonoxyhemoglobin) was crystallized with the sparse matrix approach of Jancarik and Kim (*25*) using a commercially produced screening kit (Hampton Research, Laguna Hills, CA). Using the hanging drop method, condition 4 (2.0 M ammonium sulfate and 100 mM Tris-HCl at pH 8.5) in this kit produced well-formed crystals suitable for high-resolution data collection. The unit cell parameters for these crystals (Table 1) are nearly identical to those of the high-salt, pH 7.1 crystals reported by Ladner et al. (*14*) for horse methemoglobin.

Diffraction Data Collection and Reduction. Each carbonmonoxyhemoglobin crystal was mounted in a quartz capillary tube in a nitrogen-filled glovebox, and CO was injected into the capillary immediately before sealing. In each case, a complete diffraction data set was collected from a single crystal with a Rigaku AFC6 diffractometer that was fitted with a San Diego Multiwire Systems area detector. The data were scaled and merged according to the procedure of Howard et al. (*26*). Unit cell parameters and intensity statistics are listed in Table 1.

Structure Determination and Refinement. The structure of horse carbonmonoxyhemoglobin and the structures of the three crystal forms of bovine carbonmonoxyhemoglobin all were solved by molecular replacement (*27*) with the program package MERLOT (*28*) using diffraction data between 8.0 and 4.0 Å resolution. In each case, an $\alpha 1\beta 1$ dimer of a refined structure of carbonmonoxyhemoglobin was used as the molecular replacement probe structure. For each of the three bovine carbonmonoxyhemoglobin structures, where the asymmetric unit is a tetramer, the rotation function gave only two solutions that were related by the expected dyad symmetry. The translation function uniquely positioned each rotated dimer, and the resulting $\alpha_2\beta_2$ tetramer had pseudo-222 symmetry with subunit interfaces that were stereochemically valid.

The low-pH crystal form of bovine carbonmonoxyhemoglobin, bHb·CO·PEG5.0, was the first of the bovine structures to be completed. An $\alpha 1\beta 1$ dimer from the human carbonmonoxyhemoglobin R2 structure (*20*) was used as the molecular replacement probe structure in this case. The resulting $\alpha_2\beta_2$ tetramer was refined using the stereochemically restrained least-squares program PROLSQ (*29*) with all atoms in the model initially assigned temperature factors of 20 Å^2. Refinement of this model resulted in an *R*-value of 0.24 for the 8.0−1.9 Å data set (43 783 reflections with magnitudes greater than 2.0σ). The refined atomic model, which had the amino acid sequence of human hemoglobin, was converted to a bovine hemoglobin atomic model using the program TOM/FRODO (*30*, *31*) by positioning the bovine specific residues into $F_{obs} - F_{calc}$ electron density omit maps. Water molecules were added to the structure by searching the $F_{obs} - F_{calc}$ electron density for peaks greater than 3 times the overall rms density. Putative water molecules that did not have proper stereochemistry were eliminated using the software described by Borgstahl (*32*). The final structure includes 95 water molecules and has an *R*-value of 0.196. Refinement statistics for this structure, as well as for the three structures described below, are presented in Table 1.

The bHb·CO·PEG8.5 and bHb·CO·HS7.2 crystal structures of bovine carbonmonoxyhemoglobin were solved and refined using the same general protocol described above for bHb·CO·PEG5.0. In each case, the $\alpha 1\beta 1$ dimer from the refined bHb·CO·PEG5.0 atomic model (with temperature factors reset to 20 Å^2) was used as the molecular replacement probe structure. The bHb·CO·PEG8.5 structure refined to an *R*-value of 0.189 and includes 145 water molecules. The bHb·CO·HS7.2 structure refined to an *R*-value of 0.199 and includes 118 water molecules.

In the case of the high-salt, high-pH horse carbonmonoxyhemoglobin crystal structure, eHb·CO·HS8.5, the Protein Data Bank atomic coordinates of the $\alpha 1\beta 1$ dimer of horse

Table 2: Hemoglobin Quaternary Structure Transitions[a]

transition	Δ_Q (Å)	screw-rotation axis direction angles (α, β, γ)	screw-rotation axis y-intercept (Å)	screw-rotation angle (ρ)/translation (τ)
T → hHbTm3·CO·HS6.7	4.4	1.4°, 90°, 88.6°	19.9	−10.1°/1.0 (Å)
T → hHbTm2·CO·HS6.7	4.6	−8.5°, 90°, 98.5°	21.1	−10.6°/0.4 (Å)
T → hHb·O_2·HS6.7 (T → R)	4.7	16.5°, 90°, 73.5°	13.1	−13.5°/1.5 (Å)
T → eHb·CO·HS8.5	5.2	14.8°, 90°, 75.2°	17.0	−12.8°/1.3 (Å)
T → hHbND·CO·HS6.7	5.6	37.6°, 90°, 52.4°	14.4	−13.9°/1.9 (Å)
T → hHbCA·CO·HS6.7	5.7	35.9°, 90°, 54.1°	14.1	−14.0°/1.8 Å
T → bHb·CO·HS7.2	5.8	22.1°, 90°, 67.9°	11.6	−16.6°/1.5 Å
T → bHb·CO·PEG5.0	5.9	39.3°, 90°, 50.7°	13.7	−14.9°/2.2 Å
T → bHb·CO·PEG8.5	8.1	44.0°, 90°, 46.0°	9.4	−24.0°/3.2 Å
T → hHbGII·CO·PEG8.5	8.1	47.0°, 90°, 43.0°	9.4	−23.9°/3.3 Å
T → hHb·CO·PEG5.8 (T → R2)	9.3	45.3°, 90°, 44.7°	9.2	−24.9°/3.1 Å
R → eHb·CO·HS8.5	0.9	98.5°, 90°, −8.5°	15.6	−1.6°/0.5 Å
R → bHb·CO·HS7.2	1.5	67.9°, 90°, 22.1°	7.1	−4.4°/−0.1 Å
R → bHb·CO·PEG5.0	2.5	106.4°, 90°, −16.4°	8.8	−6.5°/1.0 Å
R → hHbGII·CO·PEG8.5	3.3	89.2°, 90°, 0.8°	7.2	−8.5°/1.0 Å
R → bHb·CO·PEG8.5	3.9	84.4°, 90°, 5.6°	6.0	−10.9°/1.3 Å
R → hHb·CO·PEG5.8 (R → R2)	4.6	81.2°, 90°, 8.8°	5.8	−12.4°/1.2 Å
R2 → bHb·CO·PEG8.5	0.4	47.5°, 90°, 42.5°	4.6	1.0°/0.1 Å
R2 → hHbGII·CO·PEG8.5	1.0	71.3°, 90°, 18.7°	5.7	2.8°/−0.1 Å
R2 → bHb·CO·PEG5.0	2.4	61.5°, 90°, 28.5°	1.3	6.9°/−0.8 Å
R2 → bHb·CO·HS7.2	3.1	93.7°, 90°, −3.7°	2.5	8.3°/−1.3 Å
R2 → eHb·CO·HS8.5	4.0	80.8°, 90°, 9.2°	4.0	12.4°/−0.7 Å
bHb·CO·PEG5.0 → hHbND·CO·HS6.7	0.6	72.7°, 90°, 17.3°	2.4	1.2°/−0.3 Å
bHb·CO·PEG5.0 → hHbCA·CO·HS6.7	0.7	91.9°, 90°, −1.9°	3.2	1.9°/−0.2 Å
bHb·CO·PEG5.0 → bHb·CO·HS7.2	1.6	147.1°, 90°, −57.1°	−1.5	−3.4°/0.0 Å

[a] The parameter Δ_Q is defined in the text. The reference T, R, and R2 structures were chosen to be the hHb·DX·HS6.8 (*4*, *6*), hHb·O_2·HS6.7 (*13*), and hHb·CO·PEG5.8 (*20*) crystal structures, respectively. Structures hHbCA·CO·HS6.8 and hHbND·CO·HS6.8 were determined by Schumacher et al. (*38*). They used bis(methyl phosphate) derivatives of either 4-carboxycinnamic acid (CA) or 2,6-naphthalene dicaboxylic acid (NA) to produce two cross-linked forms of human deoxyhemoglobin that were then exposed to CO and crystallized. Both modified carbonmonoxyhemoglobins hHbCA·CO·HS6.8 and hHbND·CO·HS6.8 are cross-linked between the ϵ-NH_2 group of Lys82β1 and the ϵ-NH_2 group of Lys82β2. Structures hHbTm2·CO·HS6.8 and hHbTm3·CO·HS6.8 were determined by Schumacher et al. (*37*). They used trimesic acid (Tm) to produce cross-linked forms of human deoxyhemoglobin that were then exposed to CO and crystallized. Modified carbonmonoxyhemoglobin hHbTm2·CO·HS6.8 is cross-linked between the α-NH_2 group of Val1β1 and the ϵ-NH_2 group of Lys82β2, and hHbTm3·CO·HS6.8 is cross-linked between the α-NH_2 amino group of Val1β1, the ϵ-NH_2 group of Lys82β1, and the ϵ-NH_2 group of Lys82β2. Structure hHbGII·CO·PEG8.5 is the Grower II form of human embryonic hemoglobin and was determined by Sutherland-Smith Barker et al. (*40*).

aquomethemoglobin (*14*) were used as the molecular replacement probe structure. Prior to molecular replacement orientation and positioning, the heme groups of the horse aquomet dimer were converted to CO-liganded hemes. The eHb·CO·HS8.5 structure refined to an *R*-value of 0.178 and includes 74 water molecules per dimer.

Quaternary Structure Analysis. The following procedure was used to characterize the change in quaternary structure between pairs of refined structures as a rigid-body screw rotation (*3*, *33*). Each atomic model first was transformed to a standard orientation in which the dyad axis of the $\alpha_2\beta_2$ tetramer was positioned along the *y*-axis and the *x*-axis was aligned along the line defined by the α1Fe-β1Fe and α2Fe-β2Fe midpoints. Next the backbone atomic coordinates of the $\alpha1\beta1$ and $\alpha2\beta2$ dimers were averaged about the dyad axis for each atomic model. An iterative superposition procedure similar to the "sieve fit" procedure of Gerstein and Chothia (*34*) then was used to define a common "static core" of $\alpha1\beta1$ backbone atoms for each pair of structures being compared. Specifically, the $\alpha1\beta1$ backbone atoms of a pair of atomic models were superimposed by method of Kabsch (*35*) as implemented in the program BMFIT (*36*). A residue was defined as an outlier and omitted from subsequent superposition cycles if the rms displacement of its four backbone atoms was greater than σ times the overall rms displacement value for all backbone atoms. Initially σ was set to a value of 2.0, and the procedure was iterated until outlying residues no longer were found. At convergence, if the overall rms displacement of the remaining static core residues was greater than 0.4 Å, the process was repeated with σ decreased by 0.1. For the structures compared in this paper, the final value of σ ranged from 2.0 to 1.6, and the $\alpha1\beta1$ static core ranged in size from 157 to 268 residues. For pairings between the deoxy T structure (hHb·DX·HS6.8) and any of the fully liganded structures, the static core identified by this procedure was very similar to the invariant $\alpha1\beta1$ interface residues specified by Baldwin and Chothia in their analysis of the T and R structures (*3*). As a measure of the overall magnitude of quaternary structure difference, the parameter Δ_Q (Table 2) was defined as the rms deviation of the non-superimposed $\alpha2\beta2$ static core backbone atoms. After the $\alpha1\beta1$ dimers for a pair of structures had been superimposed, the corresponding $\alpha2\beta2$ dimers were superimposed using the same sieve fit procedure. The set of screw-rotation parameters associated with this second superposition (see Table 2) defines the quaternary structure change between a given pair of hemoglobin structures (*3*, *33*).

As mentioned above, before calculating the screw-rotation parameters for a quaternary structure transition, the coordinates of the backbone atoms of the $\alpha1\beta1$ and $\alpha2\beta2$ dimers in each tetramer were averaged about the molecular dyad to produce a tetramer with exact 2-fold symmetry. The advantage of using tetramers with backbone atoms that have exact 2-fold symmetry is that the number of independent parameters that define the rigid-body screw rotation between a pair of structures is reduced to only four. A screw-rotation

transformation is defined by the three direction angles of the screw-rotation axis (α, β, and γ), the coordinates of a point on the rotation axis, an angle of rotation about the screw axis (ρ), and a translation distance along the screw axis (τ). In general, six of these parameters are independent—two of the direction angles (since the sum of the squared direction cosines must add to unity), two of the coordinates of the point on the rotation axis (since one coordinate can be specified arbitrarily), the angle of screw rotation, and the screw translation. However, if the two tetramers each have an exact molecular dyad of symmetry, and if one of the dyads lies along the *y*-axis of the coordinate system, the screw-rotation axis must intersect and be perpendicular to the *y*-axis in order for 2-fold symmetry to be maintained. Therefore, only four independent parameters are required to uniquely specify the screw-rotation transformation in this case: one direction angle of the screw-rotation axis (α or γ since $\beta = 90°$), the *y*-intercept of the screw-rotation axis, the angle of rotation ρ, and the translation distance τ.

RESULTS AND DISCUSSION

The quaternary structure of bovine carbonmonoxyhemoglobin varies considerably in the three crystal forms described above. The low-salt/low-pH crystal form, bHb·CO·PEG5.0, does not have the quaternary R2 structure observed for human hemoglobin crystallized under very similar conditions; it has a quaternary structure that is intermediate between the R and R2 structures. A quaternary structure extremely similar to the human hemoglobin R2 structure occurs instead at higher pH in the crystal form bHb·CO·PEG8.5. The third crystal form, bHb·CO·HS7.2, has a quaternary structure that is intermediate between the R and R2 structures and is also different from that of bHb·CO·PEG5.0.

Variation in Δ_Q Values and Screw-Rotation Parameters. The Δ_Q values in Table 2 vary in magnitude from 0.4 to 9.3 Å and serve as a simple index of quaternary structure variation for the collection of hemoglobin tetramers. Defining the T, R, and R2 structures as the hHb·DX·HS6.8, hHb·O_2·HS6.7, and hHb·CO·PEG5.8 crystal structures, respectively, we can draw the following conclusions from the Δ_Q values. First, it is clear that all of the liganded tetramers have quaternary structures that differ significantly from the quaternary T structure of deoxyhemoglobin. The T versus liganded hemoglobin Δ_Q values range from a low of 4.7 Å for T vs R to a high of 9.3 Å for T vs R2. Second, the eHb·CO·HS8.5 structure is most similar to the R structure; Δ_Q is 0.9 Å for R vs eHb·CO·HS8.5 as compared to Δ_Q values of 4.0 and 4.6 Å for R2 vs eHb·CO·HS8.5 and R vs R2, respectively. Third, bHb·CO·PEG8.5 has a quaternary structure that is almost identical to R2 since Δ_Q for R2 vs bHb·CO·PEG8.5 is only 0.4 Å. Last, the other two liganded structures of bovine hemoglobin, bHb·CO·PEG5.0 and bHb·CO·HS7.2, have quaternary structures that differ significantly from each other and from the R and R2 quaternary structures. The relevant Δ_Q values in this case are 1.6 Å for bHb·CO·PEG5.0 vs bHb·CO·HS7.2, 2.5 and 2.4 Å for R vs bHb·CO·PEG5.0 and R2 vs bHb·CO·PEG5.0, respectively, and 1.5 and 3.1 Å for R vs bHb·CO·HS7.2 and R2 vs bHb·CO·HS7.2, respectively.

The second measure of quaternary structure variation is the set of four screw-rotation parameters that characterize the rigid-body transition between two hemoglobin tetramers (Table 2). This is a more complete description of quaternary structure variation in that it specifies the magnitude as well as the direction associated with the transition between two quaternary structures. The screw-rotation parameters reported in Table 2 confirm that the quaternary structure of bHb·CO·PEG8.5 is extremely similar to that of the original R2 structure, hHb·CO·PEG5.8. They also indicate that the other two liganded structures of bovine hemoglobin, bHb·CO·PEG5.0 and bHb·CO·HS7.2, are significantly different from both the R and the R2 structures.

The results of the screw-rotation calculations are schematically illustrated in Figure 1A,B where each hemoglobin tetramer is represented by two lines—one connecting the subunit centers of mass of the $\alpha1\beta1$ dimer and one connecting the subunit centers of mass of the $\alpha2\beta2$ dimer. In Figure 1A, the hHb·DX·HS6.8 (T), hHb·O_2·HS6.7 (R), hHb·CO·PEG5.8 (R2), eHb·CO·HS8.5, and bHb·CO·PEG8.5 tetramers have been aligned to the same frame of reference by superimposing the $\alpha1\beta1$ dimer of each of the four liganded structures on the $\alpha1\beta1$ dimer of hHb·DX·HS6.8. The spatial distribution of the lines representing the non-superimposed $\alpha2\beta2$ dimers illustrates the quaternary structure variation between the T, R, and R2 structures and clearly shows the very high degree of isomorphism between the hHb·CO·PEG5.8 (R2) and bHb·CO·PEG8.5 quaternary structures. The positions of the screw-rotation axes for the T → hHb·CO·PEG5.8 and T → bHb·CO·PEG8.5 transitions are essentially identical, and the positions of the $\alpha2\beta2$ dimers for the two tetramers are nearly the same. Therefore, the R2 quaternary structure is energetically accessible to both human and bovine carbonmonoxyhemoglobin despite differences in crystallization conditions, crystal lattice contacts, and primary structure. It follows that the R2 quaternary structure must exist in solutions of bovine carbonmonoxyhemoglobin under the conditions used for its crystallization (19% PEG 3350, 200 mM potassium chloride, 50 mM ammonium sulfate, and 0.1 M TAPS at pH 8.5) and solutions of human carbonmonoxyhemoglobin under the conditions used for its crystallization (16% PEG 6000, 100 mM sodium cacodylate, 75 mM chloride at pH 5.8). For the reasons discussed above, it is likely that the R2 quaternary structure is an energetically accessible structure that exists at least as a minor species for all fully liganded mammalian hemoglobins in solutions of moderate salt concentration and over a pH range of 5.8−8.5.

Although the level of quaternary isomorphism between the hHb·O_2·HS6.7 (R) and eHb·CO·HS8.5 structures is high, it is not as high as it is between hHb·CO·PEG5.8 (R2) and bHb·CO·PEG8.5. The *y*-intercepts of the T → hHb·O_2·HS6.7 and T → eHb·CO·HS8.5 screw-rotation axes differ by 3.9 Å (Table 2). In addition, the positions of the $\alpha2\beta2$ dimers for the hHb·O_2·HS6.7 and eHb·CO·HS8.5 tetramers in Figure 1A clearly differ by more than the positions of the $\alpha2\beta2$ dimers for the hHb·CO·PEG5.8 and bHb·CO·PEG8.5 tetramers. This is reflected in the higher Δ_Q value of 0.9 Å for hHb·O_2·HS6.7 vs eHb·CO·HS8.5 as compared to 0.4 Å for hHb·CO·PEG5.8 vs bHb·CO·PEG8.5 (Table 2). The original crystals of horse methemoglobin, eHb·MT·HS7.1, have the same crystal lattice as those of eHb·CO·HS8.5 but were grown under conditions of 1.5 M ammonium sulfate and 0.4 M ammonium phosphate at pH 7.1 (*22*). Signifi-

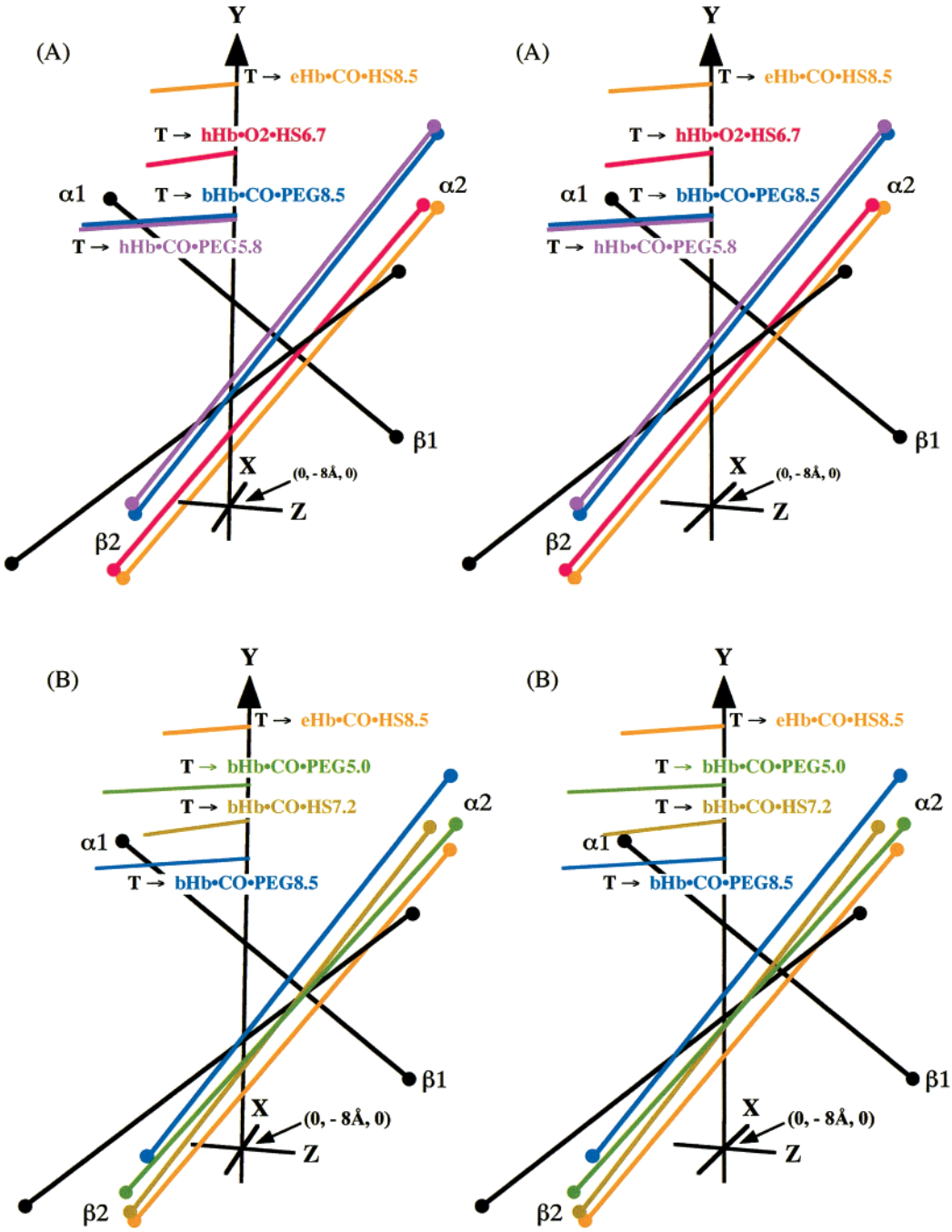

FIGURE 1: (A) Stereo diagram illustrating the rigid-body transitions between the structure hHb·DX·HS6.8 (quaternary T) and the liganded structures hHb·O_2·HS6.7 (quaternary R), eHb·CO·HS8.5, bHb·CO·PEG8.5, and hHb·CO·PEG5.8 (quaternary R2). (B) Transitions between hHb·DX·HS6.8 and the liganded structures eHb·CO·HS8.5, bHb·CO·PEG5.0, bHb·CO·HS7.2, and bHb·CO·PEG8.5. The $\alpha 1\beta 1$ and $\alpha 2\beta 2$ dimers of hHb.DX.HS6.8 are represented as black lines, and the $\alpha 2\beta 2$ dimer of each liganded hemoglobin is shown as a colored line (red, hHb·O_2·HS6.7; orange eHb·CO·HS8.5; blue, bHb·CO·PEG8.5; purple, hHb·CO·PEG5.8; brown, bHb·CO·HS7.2; green, bHb·CO·PEG5.0). The ends of each line are located at the centers of mass of the respective subunits. The hemoglobin tetramers have been positioned in a common reference frame by superimposing the $\alpha 1\beta 1$ dimer of each liganded hemoglobin on the $\alpha 1\beta 1$ dimer of hHb·DX·HS6.8. The *y*-axis is positioned along the molecular dyad of the hHb·DX·HS6.8 tetramer, and the origin of the coordinate system is located at this tetramer's center of mass. The lines perpendicular to the *y*-axis represent the screw-rotation axes for the indicated deoxyhemoglobin to liganded hemoglobin transitions.

cantly, Baldwin and Chothia (*3*) reported very similar screw-rotation parameters for the T → eHb·MT·HS7.1 transition (a *y*-intercept of 17.9 Å, $\rho = -12.3°$, and $\tau = 1.2$ Å) and for the T → hHb·CO·HS6.7 transition (a *y*-intercept of 11.9 Å, $\rho = -14.9°$, and $\tau = 0.8$ Å) as we find for the T → eHb·CO·HS8.5 and T → hHb·O_2·HS6.7 transitions, respectively, even though the eHb·MT·HS7.1 and hHb·CO·HS6.7 structures were determined at lower resolution and refined by different procedures. It would appear, therefore, that the original two "R" structures, eHb·MT·HS7.1 (or eHb·CO·HS8.5) and hHb·CO·HS6.7 (or hHb·O_2·HS6.7), actually have slightly different quaternary structures.

The two-line schematic structures of bHb·CO·PEG5.0 and bHb·CO·HS7.2 are compared with the corresponding bHb·CO·PEG8.5 and eHb·CO·HS8.5 structures in Figure 1B. It is clear from this illustration, and the data in Table 2, that

the quaternary structures of bHb·CO·PEG5.0 and bHb·CO·HS7.2 are positioned in a region that is between the R2 structure (hHb·CO·PEG5.8 and bHb·CO·PEG8.5) and the R-like structure of eHb·CO·HS8.5. On the basis of the Δ_Q values in Table 2, the bHb·CO·PEG5.0 structure is midway between R and R2, whereas the bHb·CO·HS7.2 structure is closer to R. Thus, in solution the quaternary structure of the liganded bovine hemoglobin tetramer must be a mixture of at least three energetically accessible structures. However, the stereochemical nature of the structural variation of liganded hemoglobin's $\alpha 1\beta 2$ interface (see below) suggests that it exists as an ensemble of structures (the R^e ensemble) that at a minimum varies between the R and R2 boundaries.

Additional Structures of Liganded Hemoglobin. Three crystallographic studies of crossed-linked hemoglobins (*37*−*39*) and one of human embryonic hemoglobin (*40*) also have shown that liganded hemoglobin can adopt quaternary structures between the R and R2 boundaries and in some cases outside this region. [Smith and Simmons (*41*) also have published a preliminary report of a low-salt crystal structure of human cyanomethemoglobin that adopts an R2 or R2-like quaternary structure, but refined coordinates for this structure are not yet available in the Protein Data Bank.] The data in Table 2 show that the human embryonic hemoglobin crystal structure, hHbGII·CO·PEG8.5, is another example of a mammalian hemoglobin adopting a quaternary structure that is much closer to R2 than to R. The Δ_Q values for hHbGII·CO·PEG8.5 vs hHb·CO·PEG5.8 (R2) and hHbGII·CO·PEG8.5 vs hHb·O_2·HS6.7 (R) are 1.0 and 3.3 Å, respectively. The quaternary structures of the chemically cross-linked hemoglobins hHbCA·CO·HS6.7 and hHbND·CO·HS6.7 (*38*) are very similar to the bHb·CO·PEG5.0 quaternary structure and are positioned between the R and R2 regions (Table 2). In contrast, two other cross-linked hemoglobins (*37*), hHbTm2·CO·HS6.7 and hHbTm3·CO·HS6.7, have quaternary structures that are outside the R-to-R2 range (see below). It would appear that for these two tetramers the stringent stereochemical constraints imposed by the covalent cross-links prevent access to the normal R-to-R2 region. Schumacher et al. (*37*) hypothesized that "hemoglobin intermediates, either more or less R-like, can be trapped by using cross-linkers of different lengths" and speculated that the hHbTm2·CO·HS6.7 and hHbTm3·CO·HS6.7 tetramers "represent a snapshot of the nascent R state". An extreme example of a covalent cross-link that prevents access to the normal R-to-R2 region has been reported by Kroeger and Kundrot (*39*). They determined the crystal structure of the cyanomet derivative of a recombinant hemoglobin that is cross-linked by the insertion of a single glycine residue between the NH_2-terminus of one α subunit and the COOH-terminus of the adjacent α subunit. It is clear from the data reported in their paper that this fully liganded cross-linked hemoglobin has a T-like structure.

Quaternary Variation As Illustrated in an α/ρ Plot. The magnitude of each of the four screw-rotation parameters that characterize the T → liganded hemoglobin transitions is correlated with the overall spatial displacement parameter Δ_Q (Table 2). However, the α direction angle and the screw-rotation angle ρ are the most sensitive to quaternary structure variation. Therefore, a plot of screw-rotation angle versus the α direction angle for the T → liganded hemoglobin transitions provides a two-dimensional illustration of the variation in liganded hemoglobin quaternary structures. Such a plot is shown in Figure 2 for the liganded structures reported in this paper as well as for the other recently determined structures of liganded hemoglobin discussed above. The α/ρ plot illustrates the wide quaternary separation between the R and R2 structures and shows that hHbGII·CO·PEG8.5 is another example of a mammalian hemoglobin that can adopt an R2-like quaternary structure. The quaternary structures of the cross-linked hemoglobins hHbCA·CO·HS6.7 and hHbND·CO·HS6.7 are very similar to the bHb·CO·PEG5.0 quaternary structure and are positioned between the R and R2 regions. The cross-linked hHbTm2·CO·HS6.7 and hHbTm3·CO·HS6.7 tetramers, on the other hand, have quaternary structures that clearly are outside the R-to-R2 range.

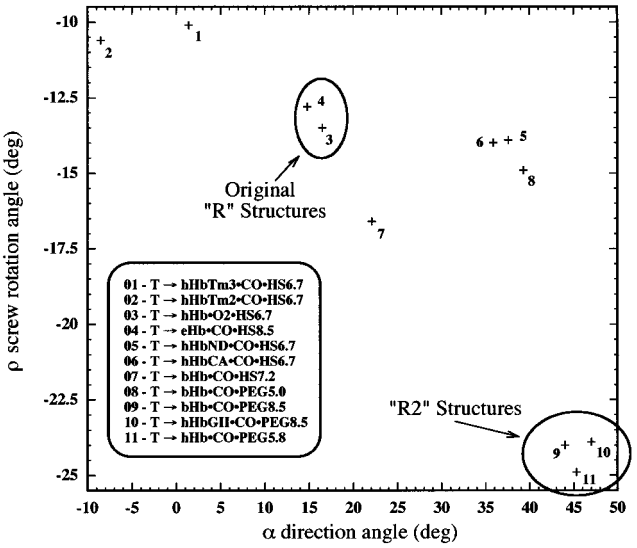

FIGURE 2: Plot of the screw-rotation angle ρ versus the α direction angle for the T → liganded hemoglobin transitions. The transitions are listed in order of the Δ_Q parameter as in Table 2.

Nature of the α1β2 Interface in Liganded Hemoglobin. The quaternary structure changes that take place as a result of the transition between deoxy and fully liganded hemoglobin are accompanied by a relatively large change in the free energy of tetramer assembly. The free energy of the dimer-to-tetramer association reaction is −14.3 kcal/mol for deoxyhemoglobin and −8.0 kcal/mol for fully liganded hemoglobin (*18*). The difference, 6.3 kcal/mol (the so-called cooperative free energy), must reflect changes in the number or strength of the interactions between αβ dimers as well as any differences in the free energy associated with ligand-induced changes in subunit tertiary structure (*42*). On the other hand, the quaternary structure differences observed in the various crystal forms of fully liganded hemoglobin most likely involve relatively small changes in free energy because they result from fairly mild changes in crystallization conditions or differences in a few surface residues. One would expect to find, therefore, only small differences in the number or strength of the dimer−dimer interactions that characterize the quaternary structures of fully liganded hemoglobin. The following analysis confirms this contention and shows that the stereochemical nature of the dimer−dimer contacts changes very little over the range of fully liganded hemoglobin structures. Interestingly, despite the small change in number and type of dimer−dimer interactions, the overall spatial displacement between the R and R2 structures (as

measured by the Δ_Q parameter or the screw-rotation angle) is almost as large as the displacement between the R and T structures.

In describing the T-to-R transition, Baldwin and Chothia (*3*) divided the $\alpha1\beta2$ interface into "switch" region residues and "hinge" region residues. They chose the term switch to describe the switching action of residues 97(FG4)β2−102(G4)β2 and the term hinge to describe the rotating motion of residues 35(C1)β2−43(CD2)β2 (Figure 3A). As a result of these translational and rotational movements, the number and nature of the noncovalent interactions in the switch and hinge regions varies considerably between quaternary T and quaternary R structures.

The exact number of noncovalent interactions at a protein−protein interface depends on the cutoff criteria used to define the direct polar and nonpolar contacts as well as the indirect water contacts. In identifying the nonbonded interactions at the $\alpha1\beta2$ interface (Figure 4 and Table 3), we have used a cutoff value of 3.5 Å for strong van der Waals contacts and 3.2 Å for hydrogen bonds (*43*). In addition, we have not counted interactions involving atoms with temperature factors greater than 40 Å^2. The last criterion was invoked in order to exclude weak interactions involving highly mobile atoms whose positions are not well defined. The weak electron density associated with these atoms reflects the fact that they are not forming strong interactions. Using these criteria, we find that the quaternary T $\alpha1\beta2$ interface (i.e., the $\alpha1\beta2$ interface of hHb·DX·HS6.8) is stabilized by seven $\alpha1/\beta2$ pairs of residues that form polar interactions (and in some cases nonpolar interactions as well) and four $\alpha1/\beta2$ pairs of residues that interact only via van der Waals contacts (Figure 4A). Together these interacting residues form a total of 7.5 polar and 13 van der Waals atomic contacts (the average of the $\alpha1\beta2$ and $\alpha2\beta1$ contacts in Table 3). In addition, the $\alpha1\beta2$ interface of the quaternary T structure includes 9 polar water bridges (Figure 3A, Figure 4A, and Table 3). In contrast, the quaternary R $\alpha1\beta2$ interface (i.e., the $\alpha1\beta2$ interface of hHb·O_2·HS6.7) is held together by just two $\alpha1/\beta2$ pairs of residues that form polar contacts and two that form van der Waals contacts (Figure 4B). These interacting residues (which are different from those stabilizing the quaternary T structure) form a total of 2 polar and 3 van der Waals atomic contacts (Table 3). (The three quaternary R water molecules shown in Figure 3C do not meet the cutoff criteria for a water bridge. Two of the three water molecules meet the distance requirements for a water bridge, but they have temperature factors that are slightly greater than the 40 Å^2.) Although the exact number of interactions in the quaternary T and quaternary R $\alpha1\beta2$ interfaces depends on the cutoff criteria, it is clear that the quaternary T $\alpha1\beta2$ interface is the stronger of the two interfaces. This conclusion is consistent with accurate thermodynamic measurements (*44*) and with the buried surface area analysis carried out by Lesk et al. (*45*).

When the same cutoff criteria are used to compare the various $\alpha1\beta2$ interfaces of the six liganded hemoglobin structures, the results suggest that all of these interfaces have similar stability. In particular, averaging over the $\alpha1\beta2$ and $\alpha2\beta1$ interfaces of six liganded tetramers yields 1.1 polar contacts, 2.6 van der Waals contacts, and 3.2 water bridges (Table 3). Moreover, the interactions are limited for the most part to the same pairs of residues (Figures 3B and 4B). All six structures include the same hydrogen bond between Asp94(G1)α1 and Asn102(G4)β2 and the same van der Waals contacts between Pro95(G2)α1 and Trp37(C3)β2. Four of the six structures include a van der Waals contact between Val96(G3)α1 and Asp99(G1)β2 (an interaction that is present in all six structure structures if the cutoff criteria are relaxed slightly). All the structures except hHb·O_2·HS6.7 have a water bridge that links backbone atoms between Arg92(FG4)α1 and Trp37(C3)β2 (cluster 3 in Figures 3C and 4B), and four tetramers have a water bridge between Asp94(G1)α1 and Asp99(G1)β2 (cluster 2 in Figures 3C and 4B). Thus, fully liganded hemoglobin can undergo a relatively large change in quaternary structure while maintaining the same small set of interactions. For the full R-to-R2 transition, the Cα atoms of residues Trp37(C3)β2, Asp99(G1)β2, and Asn102(G4)β2 shift by 1.1, 2.4, and 2.0 Å, respectively, as the β2 subunit slides relative to the α1 subunit.

In addition to the $\alpha1\beta2$ interface, the dimer−dimer interface includes the relatively weak $\alpha1\alpha2$ and $\beta1\beta2$ interfaces. In the quaternary T structure, the major interactions stabilizing the $\alpha1\alpha2$ interface involve the COOH-terminal residue, Arg141(HC3)α. Specifically, the α1 COOH-terminal carboxyl group forms a salt bridge with ϵ-amino group of Lys127(H10)α2, and the quanidinium NH1 group of Arg141(HC3)α1 forms a salt bridge with carboxyl oxygen of Asp126(H9)α2 (*2*). The cutoff criteria defined above identifies these interacting groups (and the symmetry related groups involving the α2 COOH-terminus) as the only interacting $\alpha1\alpha2$ residues. They form a total of 6 polar and 5 van der Waals atomic contacts. No water bridges form across the quaternary T $\alpha1\alpha2$ interface of hHb·DX·HS6.8. In four of the six liganded hemoglobin structures (hHb·O_2·HS6.7, eHb·CO·HS8.5, bHb·CO·HS7.2, and bHb·CO·PEG5.0), no $\alpha1\alpha2$ contacts meet the cutoff criteria. In the case of the R2 structure, hHb·CO·PEG5.8, 1 polar (a hydrogen bond between the NH_2-terminal amino group of Val1(NA1)α1 and the β-hydroxyl group of S138(H21)α2) and 1 nonpolar $\alpha1\alpha2$ interaction are detected. In the case bHb·CO·PEG8.5, 2 polar contacts [the hydrogen bond between Val1(NA1)α1 and S138(H21)α2, and another one between Ser3(A1)α1 and K139(HC1)α2], 6 nonpolar contacts, and 1 water bridge meet the cutoff criteria. No $\beta1\beta2$ interactions meet the cutoff criteria in either the T structure or in any of the fully liganded structures. [The interactions between His146(HC3)β1 and His146(HC3)β2 reported previously for hHb·CO·PEG5.8 (*20*) fall just short of satisfying the cutoff criteria in both hHb·CO·PEG5.8 and bHb·CO·PEG8.5.] Therefore, with the possible exception of a few interactions between like subunits in the hHb·CO·PEG5.8 and bHb·CO·PEG8.5, all six liganded hemoglobin tetramers are held together by essentially the same small collection of $\alpha1\beta2$ interface contacts.

In summary, the current collection of deoxy and fully liganded mammalian hemoglobin crystal structures strongly indicates that in solution the beginning and end states along hemoglobin's ligation pathway have very different quaternary structure characteristics. The deoxyhemoglobin tetramer appears to have a single energetically accessible quaternary structure, the T structure, that is held together by a relatively large set of intersubunit interactions. By contrast, the fully liganded (un-cross-linked) tetramer can sample a wide range

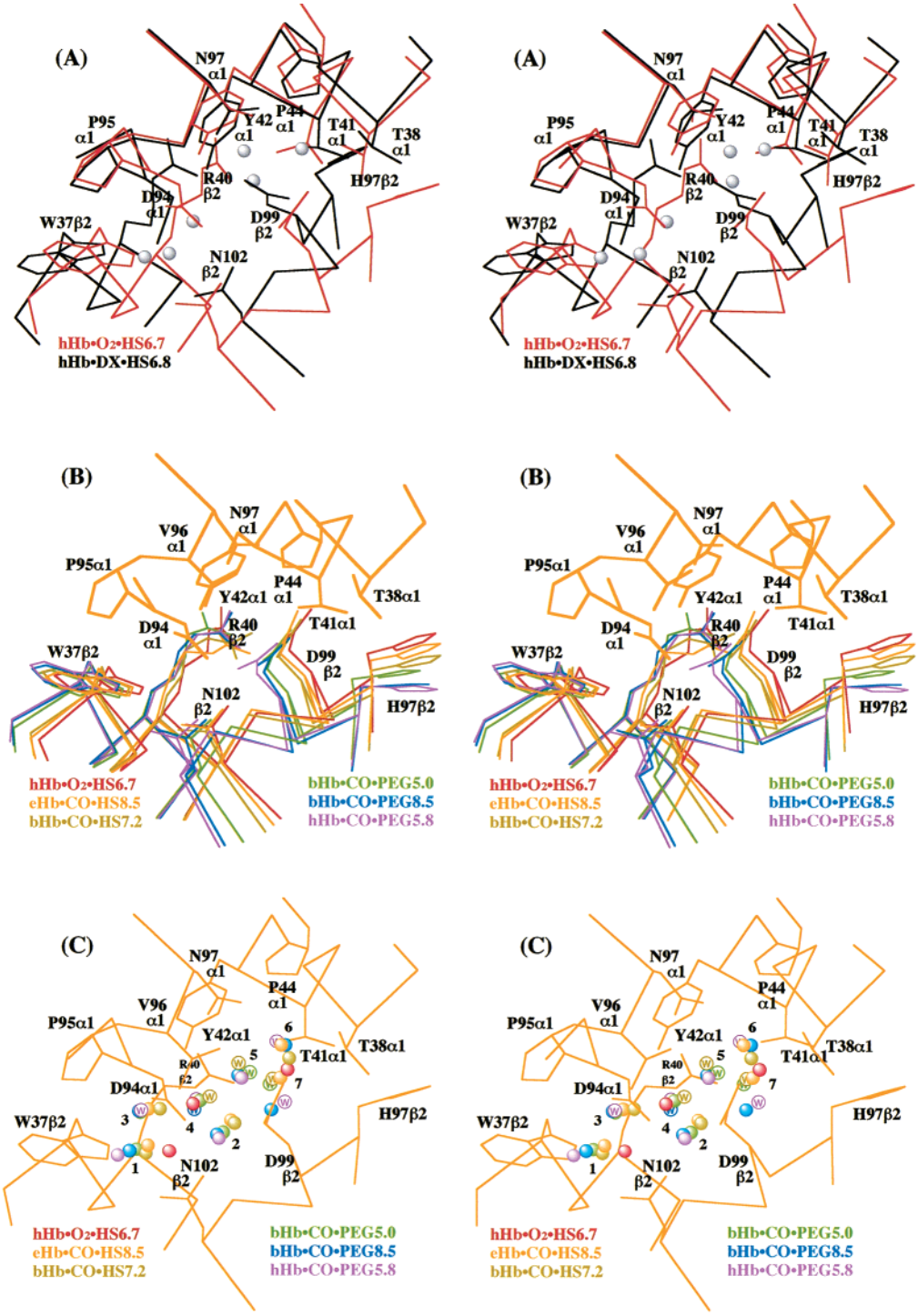

FIGURE 3: (A) Stereo diagram of the α1β2 interfaces of the hHb·DX·HS6.8 (T) and hHb·O_2·HS6.7 (R) after the backbone atoms of residues 38(C3)α1−44(CD2)α1 and 91(FG3)α1−97(G4)α1 have been superimposed. The gray spheres represent the positions of water molecules in the α1β2 interface of hHb·DX·HS6.8. (B) Stereo diagram of the α1β2 interfaces of six liganded hemoglobins (color-coded as in Figure 1) after they have been positioned in a common reference frame by superimposing the backbone atoms of residues 38(C3)α1−44(CD2)α1 and 91(FG3)α1−97(G4)α1 of hHb·O_2·HS6.7 (R), bHb·CO·HS7.2, bHb·CO·PEG5.0, bHb·CO·PEG8.5, and hHb·CO·PEG5.8 (R2) on the same residues of eHb·CO·HS8.5. For clarity, the α1 residues of only the eHb·CO·HS8.5 structure are shown. (C) Stereo diagram showing the relative positions the α1β2 interface water molecules (grouped into seven clusters and color-coded as in Figure 1) of hHb·O_2·HS6.7 (R), eHb·CO·HS8.5, bHb·CO·HS7.2, bHb·CO·PEG5.0, bHb·CO·PEG8.5, and hHb·CO·PEG5.8 (R2) overlaid on the α1β2 interface structure of eHb·CO·HS8.5. The liganded structures were superimposed as in panel B. A water molecule is represented as a filled circle if the water molecule occurs in both the α1β2 and α2β1 interfaces or by a circled W if it occurs in just one interface. Water molecules in four of the seven clusters (clusters 1, 2, 3, and 7) follow the sliding motion of the β2 residues as shown in panel B.

of quaternary structures between the R and R2 boundaries, the R^e ensemble of structures, that have relatively few intersubunit contacts. Significantly, these structural results are consistent with accurate thermodynamic data; in unliganded hemoglobin dimer-to-tetramer assembly is enthalpy driven, whereas in fully liganded hemoglobin it is driven by a large positive change in the entropy of assembly (*46*). Analysis of the liganded structures suggests that the structures of the R^e ensemble have similar stability and are linked by a simple stereochemical pathway. Specifically, the α1β2

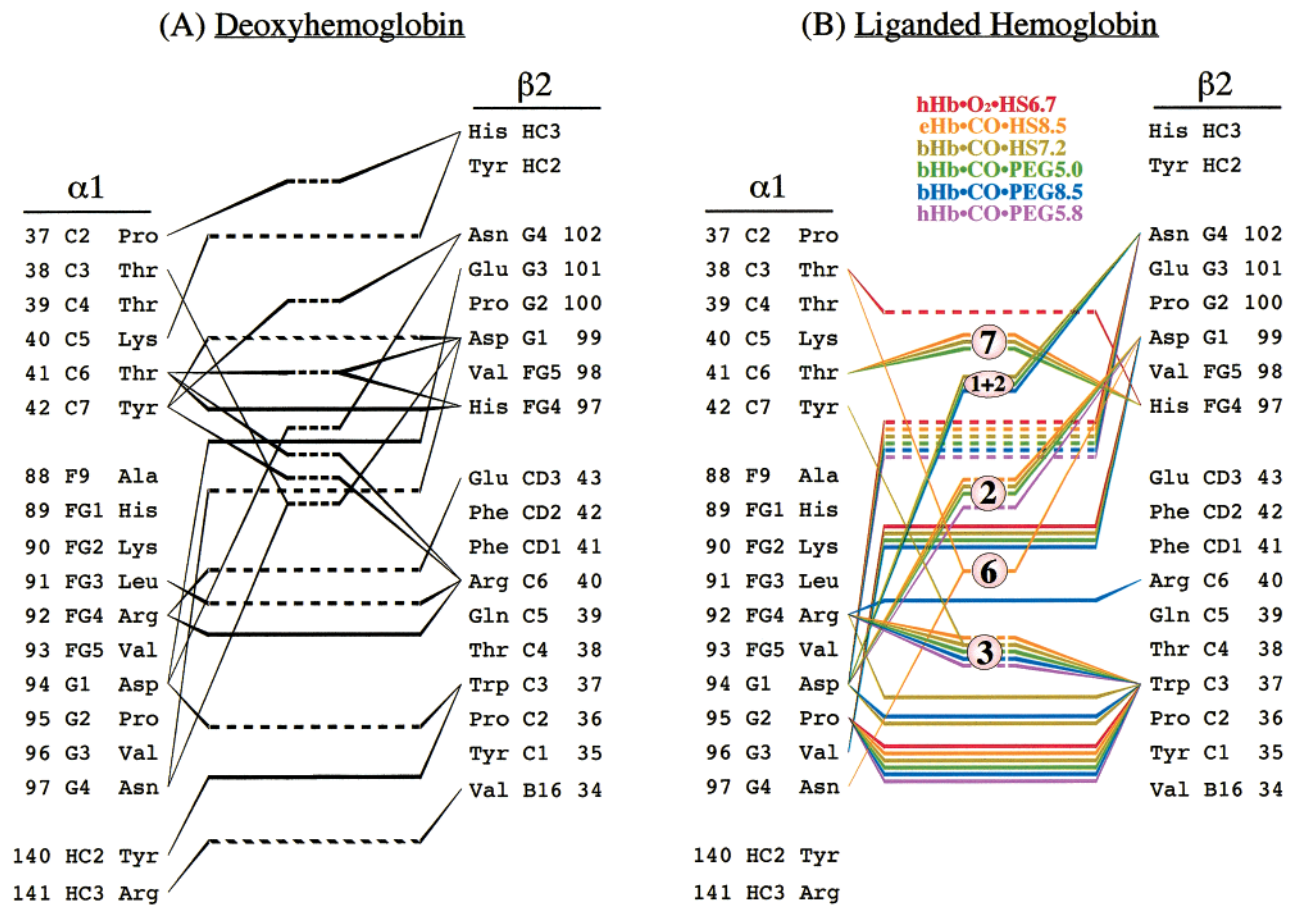

FIGURE 4: (A) Residues in contact across the α1β2 interface of the quaternary T structure, hHb·DX·HS6.8. Solid horizontal lines indicate nonpolar interactions, long dashed lines indicate polar interactions, and short dashed lines indicate water molecule bridges. (B) Residues in contact across the α1β2 interfaces of six liganded hemoglobin structures. Line definitions as in panel A. Color-coded as in Figure 1. Circled numbers refer to water clusters in Figure 3C.

Table 3: Interactions across the A1B2/A2B1 Interfaces[a]

Hb	polar contacts	nonpolar contacts	water bridges
hHb·DX·HS6.8	8/7	12/14	9/9
hHb·O_2·HS6.7	2	3	0
eHb·CO·HS8.5	1	1	6
bHb·CO·HS7.2	1/1	3/5	5/2
bHb·CO·PEG5.0	1/1	2/2	2/4
bHb·CO·PEG8.5	1/1	4/4	1/2
hHb·CO·PEG5.8	1/1	1/1	2/2
liganded Hb av	1.1 (± 0.4)	2.6 (± 1.4)	2.6 (± 1.8)

[a] For crystal structures in which the asymmetric unit is a tetramer, the number of α1β2 intersubunit contacts is followed by the number of α2β1 intersubunit contacts. For crystal structures in which the asymmetric unit is an αβ dimer, a single number specifies the number of α1β2 intersubunit contacts as well as the number of α2β1 intersubunit contacts. The following criteria were used to count the number of strong intersubunit interactions. For each type of interaction, a contact is counted only if each of the interacting atoms has a temperature factor of 40 Å^2 or less. A polar contact is defined as an atomic interaction of less than 3.2 Å between a pair of polar atoms. A nonpolar contact is defined as an atomic interaction of less than 3.5 Å between two nonpolar atoms or between a polar and a nonpolar atom. Interactions of 3.2−3.5 Å between two polar atoms are counted as nonpolar contacts. A water bridge is defined as an {α subunit polar atom−water−β subunit polar atom} ternary interaction where both hydrogen bonds are less than 3.2 Å.

interface of fully liganded hemoglobin has three main points of direct contact; the single hydrogen bond between the side chains of Asp94(G1)α1 and Asn102(G4)β2, the van der Waals contacts between the side chains of Pro95(G2)α1 and Trp37(C3)β2, and the van der Waals contacts between Val96(G3)α1 and Asp99(G1)β2. As shown in Figure 3B, these contact points act an atomic slide bearing, allowing one subunit to slide past the other. This sliding motion is also reflected in the relative positions of the water molecules that are part of α1β2 interface (Figure 3C). Starting from the hHb·O_2·HS6.7 (R) structure and moving toward the hHb·CO·PEG5.8 (R2) structure (Figure 3B), water cluster 7 shifts down as His97(FG4)β2 moves away from the region between Thr38(C3)α1 and Thr41(C6)α1, and water clusters 1−3 move from right to left as the β2 subunit slides in the same direction past the α1 subunit (Figure 3C). With a single exception, the water molecules in clusters 1−3 and 7 form all the polar water bridges across the α1β2 interface (Figure 4B). These water bridges provide "floating" points of contact that help stabilize the α1β2 interface as it shifts between the R and R2 extremes.

GENERAL IMPLICATIONS

The range of quaternary structures accessible to the fully liganded hemoglobin tetramer raises interesting questions concerning the significance of these structures to the mechanism of action of hemoglobin. In particular, there has been considerable debate over the physiological importance of the R2 structure. In a recent review article entitled "What Is the True Structure of Liganded Hemoglobin?" Tame analyzed 12 crystal structures of fully liganded vertebrate hemoglobins that are currently available in the Protein Data Bank (*19*).

He concluded that since R-like structures are much more common in this group than R2-like structures "the R state is a better representation of the oxy-Hb molecule". However, most of the R-like structures were crystallized under conditions of very high salt, whereas the R2 and R2-like structures were crystallized from PEG solutions under conditions of much lower salt concentration. For this reason, it has been suggested that the R2 structure may predominate under physiological conditions (*38*, *47*, *48*). The three new structures of bovine carbonmonoxyhemoglobin reported in this paper are consistent with this point of view. They suggest that a continuum (or a nearly continuous set) of energetically accessible structures exists for fully liganded hemoglobin between the boundaries set by the quaternary R and quaternary R2 structures and that high salt may shift the distribution toward R-like structures. The ^{19}F NMR experiments of Pearson et al. on [4-F]Trp-labeled hemoglobin provide the best direct evidence to date for the presence of abundant levels of the R2 structure in solution (*49*). They note that their observed ^{19}F chemical shifts are in "generally good agreement" with the R2 crystal structure but in "generally poor agreement" with the R crystal structure, suggesting "the existence, at least on a local scale, of [4-F]-Trp-labeled carbonmonoxyhemoglobin in the R2 state".

There also has been considerable debate over the role of the R2 structure in hemoglobin's ligation pathway. A T−R2−R pathway could provide a way around an apparent steric barrier that may exist in a direct T−R pathway (*20*). This steric barrier, as identified by Baldwin and Chothia (*3*), involves the movement of His97(FG4)β2 past Thr41(C6)α1 to its quaternary R position between Thr41(C6)α1 and Thr38(C3)α1. Simple visual analysis suggests a T−R2−R pathway as an obvious way for His97(FG4)β2 to move around Thr41(C6)α1 (Figure 3A,B). For the full R-to-R2 transition, the side chain atoms of residue His97(FG4)β2 shift an average of 3.4 Å as His97(FG4)β2 breaks a polar interaction with Thr38(C3)α1 in the R structure (Figure 4B) and moves away from the region between Thr41(C6)α1 and Thr38(C3)α1. Smith et al. (*16*) made a similar suggestion in their analysis of the Y structure of carbonmonoxyhemoglobin Ypsilanti. However, on the basis of a computer simulation using a simplified protein model in which amino acid residues were represented as spheres, Janin and Wodak (*50*) concluded that the quaternary structure observed in carbonmonoxyhemoglobin Ypsilanti lies "beyond the R state position" and suggested the possibility of a T−R−Y pathway. From a different set of computational experiments based mainly on difference distance maps, Srinivasan and Rose (*47*) reached a similar conclusion, suggesting that "the R quaternary form may lie on the pathway from T to R2". Schumacher et al. (*38*) also interpreted the results of their crystallographic studies on two cross-linked hemoglobins (hHbCA·CO·HS6.7 and hHbND·CO·HS6.7 in Table 2) in terms of a T−R−R2 pathway. In the absence of direct experimental data, however, it is probably premature to attempt to characterize the structural pathway or pathways from what appears to be a single deoxyhemoglobin quaternary T structure to the R^e ensemble of quaternary structures available to fully liganded hemoglobin. Also unanswered at present is the extent of quaternary structure variation in the eight partially liganded species (i.e., the two singly liganded, four doubly liganded, and two triply liganded liganded hemoglobin tetramers). However, it is clear that a simple two-structure equilibrium model cannot fully describe hemoglobin's mechanism of action at the atomic level. In addition to requiring both sequential (*51*) and concerted processes (*1*) [see Ackers (*52*)], cooperative ligand binding in hemoglobin also must involve equilibria between multiple quaternary structures.

With regard to the general question of the relationship between a crystal structure of an oligomeric protein and the structure of the same protein in solution, Tame comments that "The problem goes to the heart of protein crystallography: how relevant are crystal structures to the protein in solution?"(*19*). Clearly the answer to this question is that all protein crystal structures have to be viewed as structures that are energetically accessible in solution. Conversely, if a protein or any molecule, large or small, exists in solution as an equilibrium mixture of two or more structures, the process of crystallization will select (purify) from that solution one or more of these structures. A crystal structure does not necessarily represent the only structure of a protein in solution; it may represent just one member of a family of conformers. For example, Svergun et al. (*53*) have reported that the quaternary T crystal structure of aspartate transcarbamoylase is consistent with small-angle X-ray scattering measurements of the unliganded enzyme in solution. In contrast, they found that the solution scattering profile of the liganded enzyme (i.e., the enzyme complexed with N-phosphonacetyl aspartate) is not in agreement with the corresponding quaternary R crystal structure. Their analysis of the scattering data suggests that the dominant quaternary structure of liganded aspartate transcarbamoylase (in at least one set of solution conditions) may be "further away from the T structure along the reaction coordinates of the T → R transition observed in the crystals" (*53*). Thus only by solving a number of different crystal structures of the same protein can one begin to estimate the range of accessible conformations for that protein in solution.

We know of only two other examples where multiple crystal structures document a large variation in the quaternary structure of a protein. Huang et al. (*54*) determined three crystal structures of an immunoglobulin light chain dimer from a range of crystallization conditions: conditions of high salt and low pH, high salt and high pH, and low salt and neutral pH. They found considerable variation of the structure of the interface between the two variable domains of the dimer, indicating that this protein has at least three quaternary structures in solution. In the second example, Iwata et al. (*55*) reported two crystal structures of the 11-subunit bovine cytochrome bc_1 complex in which the small "Rieske" [2Fe-2S] subunit displays different subunit−subunit interactions. (However, in this case it is not known that the oxidation state of the cytochrome bc_1 complex is the same in the two crystal forms.) The only thing in common between the liganded hemoglobin tetramer, the immunoglobulin light chain dimer, and the cytochrome bc_1 complex is that they contain relatively weak interfaces that can adopt more than one energetically accessible quaternary structure. It is reasonable to assume that these three proteins are not unique in this respect. Other examples of interface variability probably are prevalent among the vast number of protein assemblies in every cell.

ACKNOWLEDGMENT

We thank Dr. Hiroshi Ueno for a sample of purified bovine hemoglobin and Dr. Eric Reinertson for a sample of bovine blood.

REFERENCES

1. Monod, J., Wyman, J., and Changeux, J.-P. (1965) *J. Mol. Biol. 12*, 88−118.
2. Perutz, M. F. (1970) *Nature 228*, 726−739.
3. Baldwin, J., and Chothia, C. (1979) *J. Mol. Biol. 129*, 175−220.
4. Fermi, G., Perutz, M. F., Shaanan, B., and Fourme, R. (1984) *J. Mol. Biol. 175*, 159−174.
5. Kavanaugh, J. S., Moo-Penn, W. F., and Arnone, A. (1993) *Biochemistry 32*, 2509−2513.
6. Kavanaugh, J. S., Rogers, P. H., Case, D. A., and Arnone, A. (1992) *Biochemistry 31*, 4111−4121.
7. Padlan, E. A., and Love, W. E. (1985) *J. Biol. Chem. 260*, 8272−8279.
8. Harrington, D. J., Adachi, K., and Royer, W. E., Jr. (1997) *J. Mol. Biol. 272*, 398−407.
9. Perutz, M. F., Fermi, G., Poyart, C., Pagnier, J., and Kister, J. (1993) *J. Mol. Biol. 233*, 536−545.
10. Tame, J. R., Wilson, J. C., and Weber, R. E. (1996) *J. Mol. Biol. 259*, 749−760.
11. Chan, N.-L., Arnone, A. unpublished.
12. Baldwin, J. M. (1980) *J. Mol. Biol. 136*, 103−128.
13. Shaanan, B. (1983) *J. Mol. Biol. 171*, 31−59.
14. Ladner, R. C., Heidner, E. J., and Perutz, M. F. (1977) *J. Mol. Biol. 114*, 385−414.
15. Perutz, M. F. (1990) *Nature 348*, 583−584.
16. Smith, F. R., Lattman, E. E., and Carter, C. W., Jr. (1991) *Proteins 10*, 81−91.
17. Doyle, M. L., Lew, G., Turner, G. J., Rucknagel, D., and Ackers, G. K. (1992) *Proteins 14*, 351−362.
18. Turner, G. J., Galacteros, F., Doyle, M. L., Hedlund, B., Pettigrew, D. W., Turner, B. W., Smith, F. R., Moo-Penn, W., Rucknagel, D. L., and Ackers, G. K. (1992) *Proteins 14*, 333−350.
19. Tame, J. R. H. (1999) *Trends Biochem. Sci. 24*, 372−377.
20. Silva, M. M., Rogers, P. H., and Arnone, A. (1992) *J. Biol. Chem. 267*, 17248−17256.
21. Perutz, M. F. (1989) *Q. Rev. Biophys. 22*, 139−237.
22. Perutz, M. F. (1968) *J. Crystal Growth 2*, 54−56.
23. Riggs, A. (1981) *Methods Enzymol. 76*, 5−29.
24. Crick, F. H. C. (1956) *Acta Crystallogr. 9*, 908−910.
25. Jancarik, J., and Kim, S. H. (1991) *J. Appl. Crystallogr. 24*, 409−411.
26. Howard, A. J., Nielsen, C., and Xuong, N. H. (1985) *Methods Enzymol. 114*, 452−472.
27. Rossmann, M. G. (1990) *Acta Crystallogr. A46*, 73−82.
28. Fitzgerald, P. M. D. (1988) *J. Appl. Crystallogr. 21*, 273−278.
29. Hendrickson, W. A. (1985) *Methods Enzymol. 115*, 252−270.
30. Cambillau, C. (1989) *Silicon Graphics Geometry Partners Directory*, p 61, Silicon Graphics, Mountain View, CA.
31. Jones, T. A. (1985) *Methods Enzymol. 115*, 157−171.
32. Borgstahl, G. E. O. (1992) Ph.D. Thesis, The University of Iowa.
33. Cox, J. M. (1967) *J. Mol. Biol. 28*, 151−156.
34. Gerstein, M., and Chothia, C. (1991) *J. Mol. Biol. 220*, 133−149.
35. Kabsch, W. (1976) *Acta Crystallogr. A32*, 922−923.
36. Yuen, P. S., and Nyburg, S. C. (1979) *J. Appl. Crystallogr. 12*, 258.
37. Schumacher, M. A., Dixon, M. M., Kluger, R., Jones, R. T., and Brennan, R. G. (1995) *Nature 375*, 84−87.
38. Schumacher, M. A., Zheleznova, E. E., Poundstone, K. S., Kluger, R., Jones, R. T., and Brennan, R. G. (1997) *Proc. Natl. Acad. Sci. U.S.A. 94*, 7841−7844.
39. Kroeger, K. S., and Kundrot, C. E. (1997) *Structure 5*, 227−237.
40. Sutherland-Smith, A. J., Baker, H. M., Hofmann, O. M., Brittain, T., and Baker, E. N. (1998) *J. Mol. Biol. 280*, 475−484.
41. Smith, F. R., and Simmons, K. C. (1994) *Proteins 18*, 295−300.
42. LiCata, V. J., Dalessio, P. M., and Ackers, G. K. (1993) *Proteins 17*, 279−296.
43. Creighton, T. E. (1993) *Proteins*, W. H. Freeman, New York.
44. Ackers, G. K. (1980) *Biophys. J. 32*, 331−346.
45. Lesk, A. M., Janin, J., Wodak, S., and Chothia, C. (1985) *J. Mol. Biol. 183*, 267−270.
46. Mills, F. C., and Ackers, G. K. (1979) *J. Biol. Chem. 254*, 2881−2887.
47. Srinivasan, R., and Rose, G. D. (1994) *Proc. Natl. Acad. Sci. U.S.A. 91*, 11113−11117.
48. Huang, Y., Koestner, M. L., and Ackers, G. K. (1997) *Biophys. Chem. 64*, 157−173.
49. Pearson, J. G., Montez, B., Le, H., Oldfield, E., Chien, E. Y., and Sligar, S. G. (1997) *Biochemistry 36*, 3590−3599.
50. Janin, J., and Wodak, S. J. (1993) *Proteins 15*, 1−4.
51. Koshland, D., Nemethy, G., and Filmer, D (1966) *Biochemistry 5*, 364−385.
52. Ackers, G. K. (1998) *Adv. Protein Chem. 51*, 185−253.
53. Svergun, D. I., Barberato, C., Koch, M. H., Fetler, L., and Vachette, P. (1997) *Proteins 27*, 110−117.
54. Huang, D., Ainsworth, C. F., Stevens, F. J., and Schiffer, M. (1996) *Proc. Natl. Acad. Sci. U.S.A. 93*, 7017−7021.
55. Iwata, S., Lee, J. W., Okada, K., Lee, J. K., Iwata, M., Rasmussen, B., Link, T. A., Ramaswamy, S., and Jap, B. K. (1998) *Science 281*, 64−71.

BI0012944